Int. J. Electrochem. Sci., 11 **(2016)** 2153 - 2165

International Journal of
ELECTROCHEMICAL
SCIENCE
www.electrochemsci.org

Preparation and Electrochemical Properties of Multiscale Porous Active Carbon for Supercapacitor Electrodes Made from Ultra-Pure Lignite by Microwave Irradiation

Mingyue Zhang[1], *Xing Zhao*[2,3] , *Quanchao Zhuang*[2,*]

[1]Department of Materials Science and Engineering, College of Earth and Mineral Sciences at The Pennsylvania State University, University Park, PA 16802,USA
[2]Lithium-ion Batteries Laboratory, School of Materials Science and Engineering, China University of Mining and technology, Xuzhou 221116, China
[3]School of Chemical Engineering and Technology, China University of Mining and technology, Xuzhou 221116, China
[*]E-mail: zhuangquanchao@126.com, qzhuang4@uwo.ca

Received: 11 November 2015 / *Accepted:* 19 December 2015 / *Published:* 1 February 2016

Multiscale porous activate carbon with appropriate pore-size distribution for supercapacitor electrode was prepared from ultra-pure lignite with only 0.3wt% ash through the synergistic effect of microwave irradiation, the activation of KOH and $ZnCl_2$, ultra-fine grinding and surface modification with sodium dodecyl benzene sulfonate(SDBS) on active carbon. The active carbon sample was characterized using laser particle size analyzer and specific surface area and pore size analyzer. Electrochemical properties of active carbon were investigated using cyclic voltammogram(CV), electrochemical impedance spectroscopy(EIS) and galvanostatic charge-discharge test with the electrolyte of 6M KOH solution.. The results show that the active carbon obtained at the conditions of microwave irradiation power of 700W, microwave irradiation time of 6minutes and weight ratio of 1:2:3(Lignite/$ZnCl_2$/KOH) has high specific surface area($1536m^2 \cdot g^{-1}$) and large percentage of micropores (59.05%). When the active carbon is ultra-fine grinded to an average size of 2.1μm, the specific surface area will be improved to $1696m^2.g^{-1}$. Active carbon treated with ultra-fine grinded and surface modification using SDBS presents a high specific capacitance of $189F \cdot g^{-1}$ and good cycle stability in KOH electrolytes.

Keywords: Supercapacitor, Multiscale porous active carbon, Electrochemical properties, Microwave irradiation, Lignite

1. INTRODUCTION

Supercapacitors have high capacitance benefited from using porous carbon as electrode material. Active carbon is the most commonly used one among various electrode carbon materials for supercapacitors due to its high-specific surface area, highly porous structure, good electrical conductivity, high chemical stability, abundent resource and relatively low cost[1,2]. However, although the high surface area and porosity of active carbon would bring a high capacitance of supercapacitors, the specific capacitance is not always in directly proportional to the surface area, someone thinks that some micropores in active carbon have too small pore size to let the electrolyte ion enter in, the surface area of this part of micropores is useless because it has no contribution to capacitance, and the smaller the average pore size of active carbon, the greater the useless specific surface area accounted for the proportion of total surface area[3]. However, the mesoporous carbon by template method which has plenty mesopores, which are larger than micropores, but has not made big breakthroughs in specific capacitance[1,4]. More and more research results show that the porous carbon with various pore widths presents higher specific capacitance because of of the ability to combine advantages of different pores. Big pores serving as cache pool for electrolyte ions can decrease the diffusion distance of electrolyte ion. Mesopores may provide lower resistance transport channels for electrolyte ions, and micropores may enhance the double-layer capacitance[1,5,6].

In this paper, the main aim is to prepare multiscale porous active carbon for supercapacitors with appropriate pore-size distribution, high micropore volume and relatively high percentage of mesopores through the synergistic effects of selecting ultra-fine grinded and ultra- purified lignite from Indonesia as feed coal, using microwave irradiation method, selecting KOH and $ZnCl_2$ both as activation agents, and the prepared active carbon was ultra-fine grinded and surface modified. Then the physical and electrochemical properties of the active carbon with different processing conditions are studied here.

2. EXPERIMENTAL PART

2.1 The pretreatment of feedstock for active carbon

Low-rank coal has abundant primitive pores, high volatile and high reactive activity. In the carbonization and activation process, its carbon skeleton structure easily develop to amorphous carbon structure with more mesopores and micropores[7-9], which may form multiscale porous structured active carbon easily.

Lignite from Indonesia with 5.6% ash and 40.55% volatile component is the feedstock here. The feed lignite was dry ultra-fine grinded using high frequency vibration mill for 1 hour with the vibration frequence is 50Hz, grinding media (stainless steel powder) size of less then 1mm and filling ratio of 40%. The ultra-fine grinded lignite was characterized using laser particle size analyzer (Jingxin, JL-1197, Chengdu, China).

Minerals associated with the feed lignite can not only weaken the activation reaction intensity, but also degrade the quality and performance of active carbon[7,10], so the feed lignite was ultra-fine grinded to liberate minerals firstly. Then the ultra-grinded lignite was firstly wet using trace ethanol before fully impregnated in 1:1 HCl for 24h to remove carbonate and lots of sulphate, then was filtered and washed with deionized water to pH=6. The HCl-treated lignite was further fully impregnated in

1:1 hydrofluoric acid (HF) for 24h to remove silicate minerals[11], then was filtered and washed with deionized water to pH=6 and dried at 105°C for 6h. Finally, the ultra-pure feedstock lignite for active carbon was prepared.

2.2 Preparation and characterization of active carbon materials

KOH is one of the most commonly used effective activation agent, the active carbon through the activation of KOH has abundant micropores, meanwhile, $ZnCl_2$ is another commonly used activation agent, and active carbon made through $ZnCl_2$ activation has abundant mesopore[12]. So we select both KOH and $ZnCl_2$ as activation agents in order to prepare multiscale porous active carbon with appropriate pore-size distribution, high micropore volume and relatively high propotin of mesopores.

The ultra-pure lignite with KOH and $ZnCl_2$ as the activation agent were mixed together at various weight ratios using deionized water as a solvent under vigorous stirring in order to mix homogenously. After 6 hours' standing at room temperature, the mixture was dried at 105°C in drying oven for 24 h, then the dried and caked sample was regrinded to less then 0.074mm.

Then, we adapted microwave irradiation method in the carbonization and activation process. Compared with traditional heating methods, microwave irradiation heating has advantages of fast speed, high efficiency, uniform heating, high efficiency of energy conservation, easy to operate and easy to automatically control[13,14].

The impregnated sample (weighing 10g for every experiment) was carbonized and activated in microwave reactor (GalanzT70D20TR-D4 microwave oven, Shunde, China) for various time with irradiation power of 700 W under N_2 flow of $300ml\cdot min^{-1}$. Then, it was cooled under N_2 flow to room temperature. The carbonized and activated samples were fully impregnated in 1:1 HCl for 24h, then was filtered and washed with deionized water to pH=6, subsequently, the HCl-treated lignite was further fully impregnated in 1:1HF for 24h to remove excess KOH and $ZnCl_2$[15], then was filtered and washed with deionized water to pH=6. The final active carbon product was dried at 105°C for 6h.

Firstly, the lignite/$ZnCl_2$/KOH mixture with the mixing weight ratio of 1:2:3 under the microwave irradiation time of 2min, 4min, 6min, 8min and 10min were conducted, respectively, The resultant activated carbons were labeled as 1#, 2#, 3#, 4#, 5#, respectively. Surface area pore size analyzer（Beishide, 3H-2000PM1, Beijing, China）was used to characterize the surface area and pore structure of the active carbon samples using N_2 sorption under 77.3K. The samples were degassed at 150°C for 5h before measurements. Brunauer–Emmett–Teller (BET) and Barrett–Joyner–Halenda (BJH) models were used to determine the specific surface areas and the pore sizes of the samples, respectively. From the tests result above we optimized the irradiation time, then the experiments of mixing weight ratio of Lignite/$ZnCl_2$/KOH of 1:1:3 and 1:3:3 were conducted, the resultant activated carbons were labeled as 6# and 7#. Then, we selected the best active carbon sample with highest specific surface area and high micropore volume and relatively high percentage of mesopore from 1#, 2#, 3#, 4#, 5#, 6# and 7# samples to be dry ultra-fine grinded using high frequency vibration mill for 5h with the vibration frequence is 50Hz, grinding media (stainless steel powder) size of less then 1mm and filling ratio of 40%. The ultra-fine grinded best active carbon was characterized with laser particle size analyzer, specific surface area and pore size analyzer.

2.3 Preparation of active carbon electrode and assembling of the supercapacitor

The active carbon electrode used in this study was prepared by spreading a mixture comprising, by weight, 75 wt% active carbon, 20 wt% graphite (Shanshan limited Co. Shanghai, China) and 5 wt% polytetrafluoroethylene (PTFE) binder dissolved in N-methyl-2-pyrrolidone (NMP, Alfa Aaesar, A. Johnson Matthey Company, China) with isopropyl alcohol as the dispersing agent onto a foamed nickel foil as the current collector. The mixture was ultrasonicated for 30min to obtain a homogeneous dispersity before spreading. The electrode were cut into wafer and made a tabletting after 50℃ forced air drying for 6h, then dried them in vacuum drying oven with 120℃ for 24h. Before assembling the coin supercapacitor, the electrodes are soaked in the electrolyte (6 M KOH) for 24h.

2.4 Electrochemical test of supercapacitor

CV and EIS were carried out by an electrochemical workstation (CHI660D, Chenhua Co., Shanghai, China) at room temperature. Charge-discharge test was evaluated using CR2032-type coin capacitor and charged and discharged in a battery analzyers (2XZ-2B, LANHE, Wuhan, China) over a range of 0-0.8 V. The weight capacity of the single electrode ($F\cdot g^{-1}$) is counted by the straight line part in the discharge process of charge/discharge curve using equation (1)[16-18]:

$$Cp = \frac{4i\Delta t}{wm\Delta U} \qquad (1)$$

Where i, Δt, w, m, and ΔU represent the current (A) of discharge process, time (s), the mass fraction of active carbon, the weight of the double electrodes and potential changes (V), respectively.

3. RESULTS AND DISCUSSION

3.1 Feedstock properties

Fig.1 shows the size distribution of ultra-fine grinded lignite. It can be seen that the feedstock lignite has been ultra-fine grinded to less than 100μm, the average size is 23.8μm, and most of associated minerals have been liberated in such size scale. The ash content of ultra-pure lignite was reduced from 5.6% to 0.3% through acid dipping treated to remove minerals.

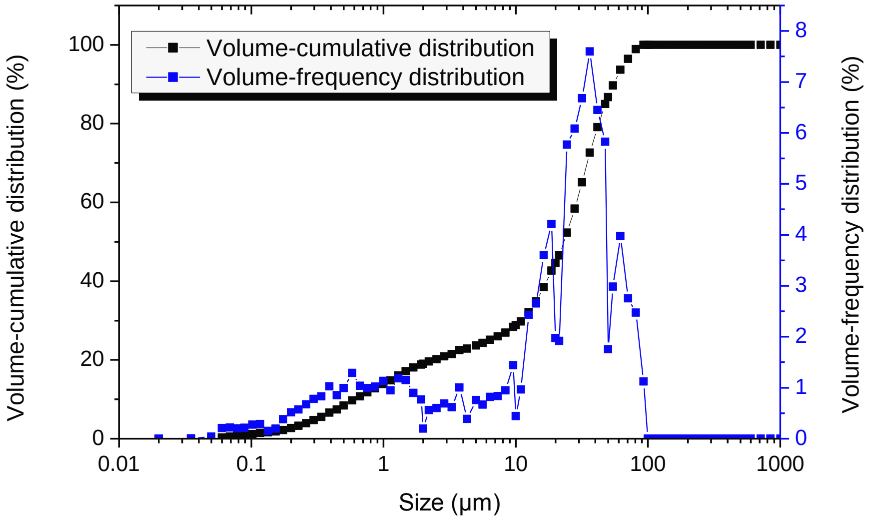

Figure 1. Size distribution of feedstock

3.2 Preparation and characterization of active carbon materials

3.2.1 The influence of irradiation time on properties of active carbon

Table 1 shows the properties of active carbons obtained from various microwave irradiation time under the condition that the mixing weight ratio of Lignite/$ZnCl_2$/KOH is 1:1:3.We can clearly observe that when microwave irradiation time is 2min, the specific surface area of 1# sample is $1079m^2 \cdot g^{-1}$, the total micropore volume is $0.7095ml \cdot g^{-1}$, the percentage of micropore is 56.03%, the average pore diameter is 2.63nm, and the yield is 52%.

Table 1. Properties of active carbons obtained from various microwave irradiation time

Sample	Irradiation time /min	S_{bet} /$m^2.g^{-1}$	V_t /$ml.g^{-1}$	V_{mic} /$ml.g^{-1}$	V_{mic} /V_t /%	D_v /nm	Yield /%
1#	2	1079	0.7095	0.39753	56.03	2.63	52
2#	4	1095	0.9028	0.36391	40.31	3.30	42
3#	6	1536	0.9298	0.54909	59.05	2.42	36
4#	8	1409	0.9220	0.53554	58.09	2.62	30
5#	10	1264	0.8380	0.44513	53.12	2.65	25

Along with the microwave irradiation time extends to 4min, the specific surface area has a few increase, but total micropore volume of 2# sample increases to $0.9028\ ml \cdot g^{-1}$ with a increase of 27.3%, the percentage of micropore decrease to 56.03%. This should be related to the raise of reaction temperature and the enhancement of function of the activator which can causes the mesopores got fully developed, then the total micropore volume increases and the percentage of micropore decrease. It can also be proved from the increase of average pore size from 2.63nm to 3.3nm.

Along with the microwave irradiation time extends to 6min, the reaction temperature further increases and more reactions of KOH with carbon atoms especially with the atoms on the face of new mesopores come into being, then more micropores form at the positions of C atoms. During the reaction process, the reactions expend C and produce CO to form more micropores on one hand, and generate kalium on the other hand. When the reaction temperature reach the boiling point of kalium, the gaseous kalium travels though the crystallite layer and splits the Aromatic lamella, then creates more new micropores[19]. Therefore, the specific surface area of 3# sample rapidly improves to 1536$m^2 \cdot g^{-1}$, meanwhile, the total micropore volume improves to 0.9298$ml \cdot g^{-1}$ and the percentage of micropore improves to 59.05 % by a large margin, the average pore diameter decreases to 2.42 nm as the increase of percentage of micropore, on the contrary, the yield decrease to 36%.

As the irradiation time extending to 8min and 10min, the specific surface area and percentage of micropore of 4# and 5# samples decrease and average pore diameter increase because the too higher reaction temperature can causes the excessive ablation of carbon, then causes the collapse of micropores. Finally, the optimized irradiation time is 6min.

3.2.2 The influence of weight ratio of Lignite/$ZnCl_2$/KOH on the properties of active carbon

On the basis of the above experiment results, the experiments of different weight ratio of Lignite/$ZnCl_2$/KOH on the properties of active carbon were investigated with the irradiation time of 6min, the results are shown in Table 2.

The active carbon samples corresponding to the weight ratio of Lignite/ZnCl2/KOH of 1:1:3 and 1:3:3 were labeled as 6#, 7# respectively. Obviously, the specific surface area and percentage of micropore of 6# sample and 7# sample are inferior to that of 3# sample. So, we use 3# sample to finish all following electrochemical tests. Besides, 3# sample was relabeled as AC-1 in the following experiments.

Table 2. Properties of active carbons of different weight ratio of Lignite/$ZnCl_2$/KOH

Sample	Coal:$ZnCl_2$:KOH	S_{bet} /$m^2.g^{-1}$	V_t /$ml.g^{-1}$	V_{mic} /$ml.g^{-1}$	V_{mic} /V_t /%	D_v /nm
$6^{\#}$	1:1:3	1491	1.0307	0.52756	51.18	2.76
$7^{\#}$	1:3:3	1516	1.0658	0.52686	49.43	2.81

3.2.3 The influence of the size of active carbon on the properties of active carbon

The AC-1 sample was ultra-fine grinded, and then the ultra-fine grinded AC-1 sample was labeled as AC-2. The AC-2 sample has a very small average size (D_{50}=2.11μm). Fig.2 shows the size distribution of AC-2 sample, it can be seen that almost all active carbon particles are less than 4μm, the size of submicron meters. The ultra-fine grinding brings active carbon particle an increase of external surface area, and the total specific surface area of AC-2 has increase to 1696$m^2 \cdot g^{-1}$ with a increase of

10.4% compared to AC-1 sample. Meanwhile, the size decrease of active carbon particle shortens the electrolyte ion diffusion distance in micropores.

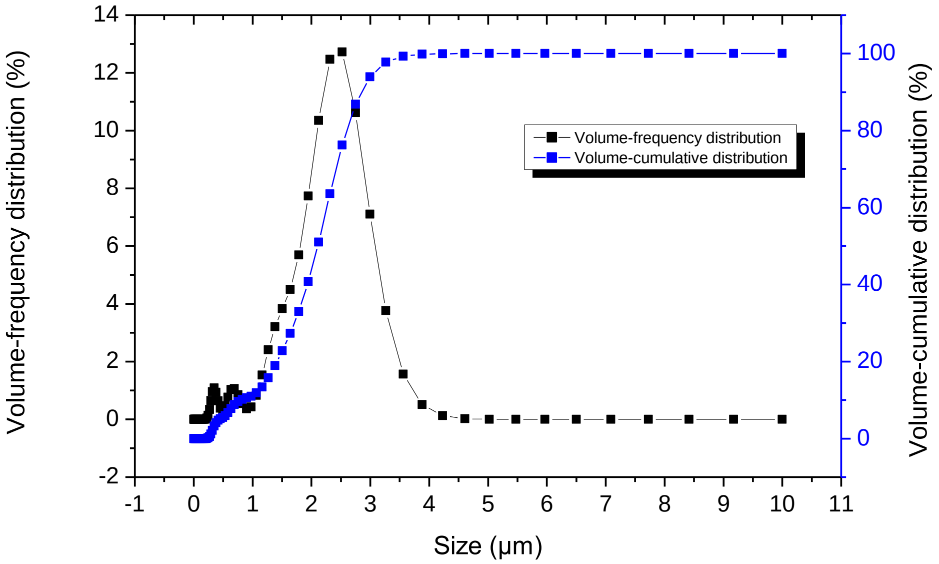

Figure 2. Size distribution of AC-2 sample

The pore width distribution of AC-2 sample is given in Fig.3. The peaks indicate that the pores are mainly micropores with diameter of about 1 nm and mesopores with diameter of about 3.5 nm, the average pore diameter is about 2.64nm. This kind of multiscale porous active carbon supplies appropriate pore-size distribution, has little useless specific surface area, its mesopores may provide low resistance transport channel for electrolyte ion, and micropore may enhance the double-layer capacitance, and the space among submicro-scale active carbon particles serves as cache pool for electrolyte ion can improve the electrochemical stability of electrode.

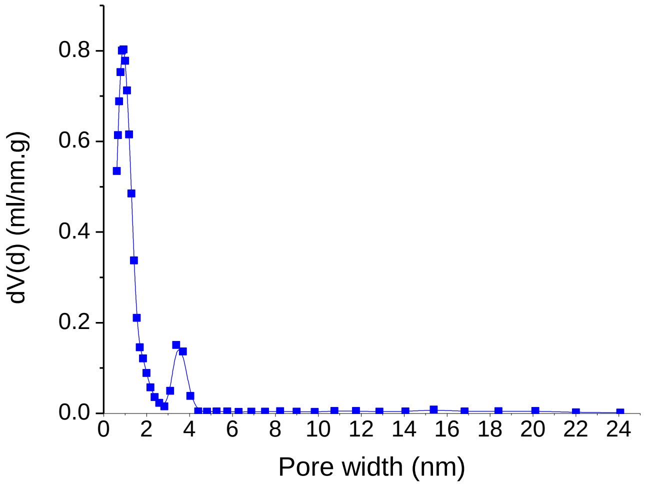

Figure 3. Pore width distribution of AC-2 sample

3.3 The electrochemical performance of active carbon based supercapacitor

In order to deeply study the impact of the property of active carbon on the performance of supercapacitor, surface modification with sodium dodecyl benzene sulfonate (SDBS) which can improve the wettability and electrochemical properties of active carbon[20] has been done on the sample AC-2 and the new sample is named AC-3. Then electrochemical performances test were carried out on the sample AC-1, AC-2 and AC-3, respectively. Fig.4 shows the initial 30 CVs from 0V to 0.8 V with the scan rate of 1mV·s^{-1} for the three kinds of samples, respectively. As can be seen, the coincidences are all very well for the three kinds of samples, which indicated that all the samples have stable cycling performance. There are no obviously redox peaks in CV curves with the voltage range of 0-0.8 V, which indicated that the capacity of the supercapacitor all provide by the double layer capacity. The area of the CV curve for the ultra-fine grinded sample AC-2 is much larger and closer to the rectangular shape than that of AC-1 without ultra-fine grinded, indicating that the ultra- fine grinded can both improve the capacity and reversibility of active carbon. Then as the fine grinded active carbon has been done the surface modification with SDBS, shown in AC-3, its CV curves almost become a rectangular shape, and has a more larger area, which indicated that surface modification can improve the wettability of electrode and compatibility between electrode and electrolyte, increase the capacity of the electrode, decrease the resistance and improve the cycling performance of the supercapacitor.

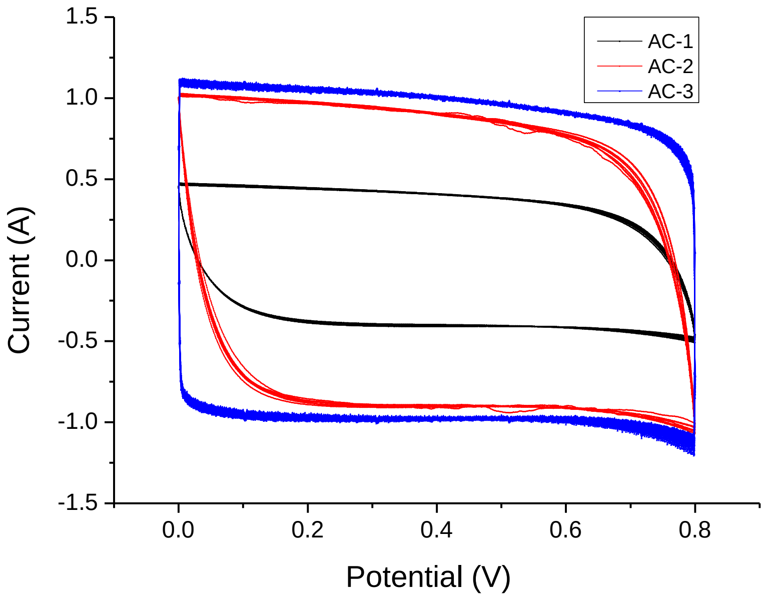

Figure 4. CV curves of various electrodes

Fig.5, Fig.6 and Fig.7 show us the first charge-discharge curve with different current density (20mA·g^{-1}, 50mA·g^{-1}) of AC-1, AC-2 and AC-3, respectively. As can be seen, the charge-discharge curves of the three kinds of samples all show an approximate isosceles triangle, which indicated the supercapacitors with active carbon as the electrodes have a typical double layer capacitor characteristics and there is almost no faraday current caused by the redox reactions. The capacity is

170F·g^{-1} for AC-1, 184F·g^{-1} for AC-2 and 18 F·g^{-1} for AC-3 with the current density of 20mA·g^{-1}. The ultra-fine grinded active carbon shows the highest capacity, which is coincided with the CV results. However, with the current density increasing to 40mA·g^{-1}, the capacity of the three samples all decrease, which show that the capacity of AC-1 decrease to 120F·g^{-1} with a drop of 29%, AC-2 decrease to 175F·g^{-1} with a drop of 4.9% and AC-3 decrease to 182F·g^{-1} with a drop only of 3.7%. The results above show us that the ultra-fine grinded active carbon has the best capacity and rate performance.

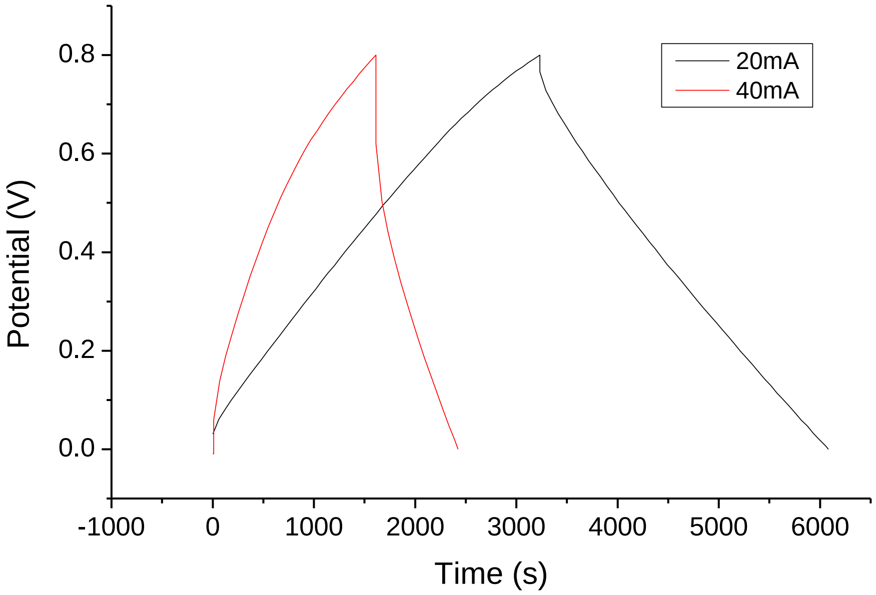

Figure 5. Charge/discharge curves of AC-1

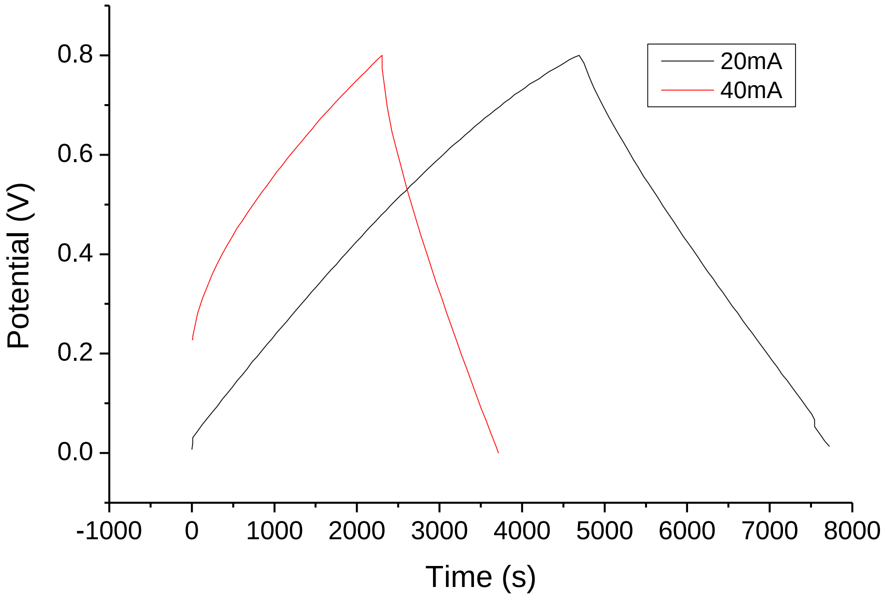

Figure 6. Charge/discharge curves of AC-2

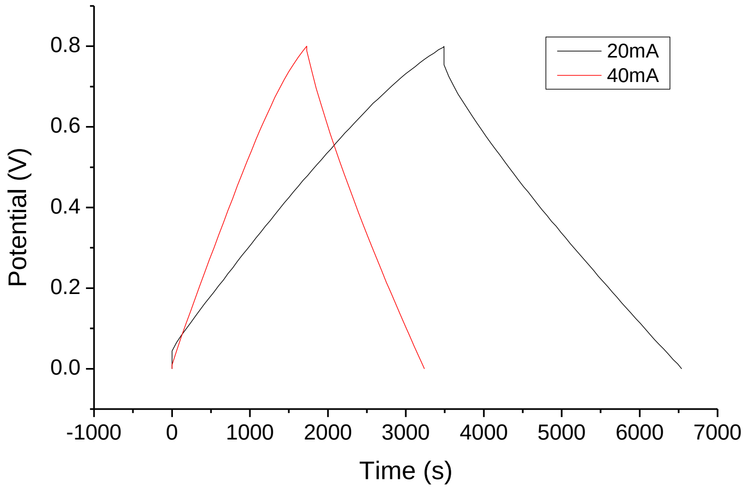

Figure 7. Charge/discharge curves of AC-3

Fig.8 shows us the cycling performance of the three samples. As can be seen, the supercapacitor with AC-1 as the electrodes shows much faster capacity fading than that of AC-2 and AC-3. However, the supercapacitors with AC-2 and AC-3 as the electrodes show well cycle stability with the capacity drop less than 5% even after 380 cycles.

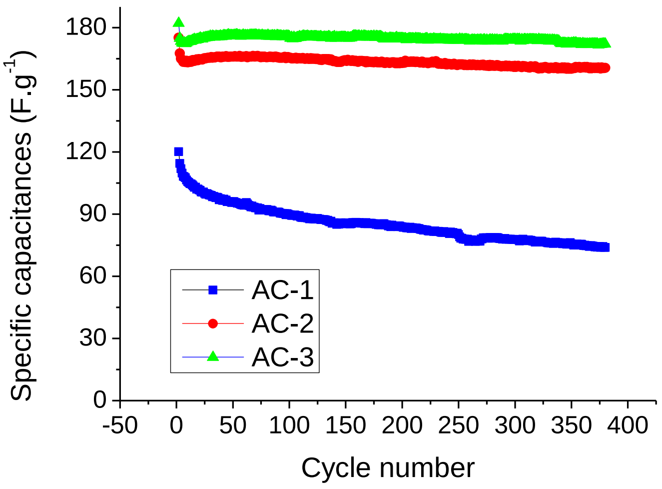

Figure 8. Cycling performance of various electrodes

Fig.9 shows us the Nyquist plots of the three electrodes. As can be seen, all the plots illustrate a semicircle and inclined line at high and low frequency regions, respectively. The semicircle at the high frequency range represents the equivalent series resistance (ESR) as the total resistance in the system, which includes the electrolyte resistance, contact resistance (i.e., between the carbon particles at the current collector/carbon film interface), and intrinsic resistance of components (i.e., current collectors and carbon)[21,22].

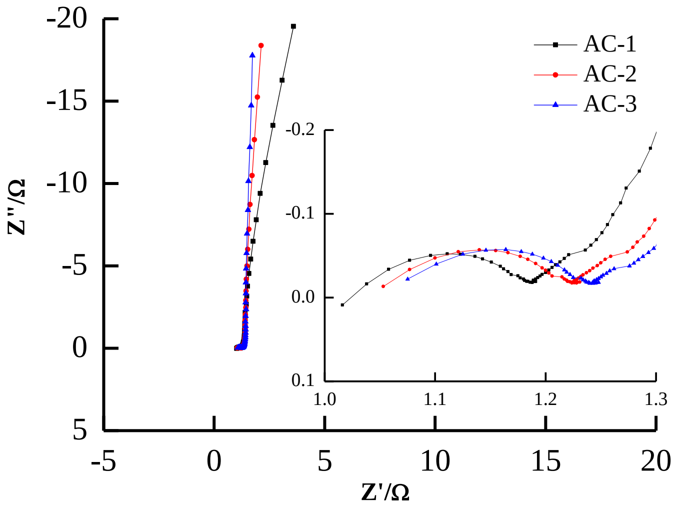

Figure 9. Nyquist plots of the three electrodes

According to the experimental results obtained in this work, an equivalent circuit, as shown in Fig.10, is proposed to fit the impedance spectra shown in Fig. 9. The resistance-capacitance (RC) circuit signifies the semicircle in the Nyquist plots of the EIS. CPE is a constant phase element, and CPE is used instead of capacitance in this study. R_s is the Ohmic resistance; R_E is the ESR; Q_{dl} represent the double-layer capacitance in the high-frequency region. The low-frequency region, however, cannot be modeled properly by a finite Warburg element. We have chosen, therefore, to replace the finite diffusion by a CPE, that is, *W*.

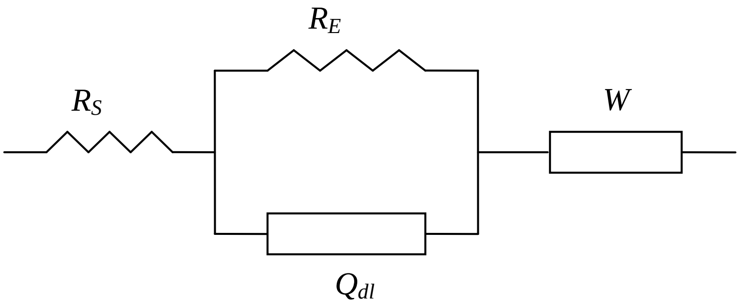

Figure 10 Equivalent circuit proposed for fitting impedance spectra shown in Fig. 9

The fitting result of the semicircle in high frequency region is shown in Fig. 11. As can be seen, the three electrodes all have a low resistance value which reflects high rate of electron transfer and keep the electrochemical activity of supercapacitor[23]. For supercapacitor, the low frequency range of EIS should shows a line near 90° with real axis which indicates there is no redox reaction on the interface between the electrode and electrolyte. As shown in Fig 9, the line of AC-3 more inclined to the real axis near the 90° ideal value at the low frequency range than AC-2 and AC-1 corresponds to the K^+ diffusion into the bulk of the electrode material. This scenario indicates a suitable capacitive behavior without a redox reaction that has appropriate correlation with the CV results. And the resistance of the supercapacitor with AC-3 as electrode material, which is the point of intersection of Nyquist plots and the real axis, is only 1.4Ω[24,25].

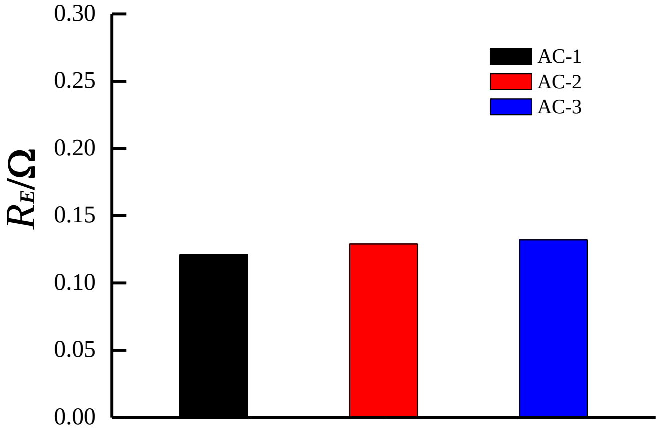

Figure 11 The R_E of different electrodes

4. CONCLUSIONS

(1) The ultra-pure lignite with only 0.3% ash content was prepared through acid dipping treated to remove minerals. Activated carbon with a specific surface area of $1536m^2 \cdot g^{-1}$, total pore volume of $0.9298ml \cdot g^{-1}$, and especially the larger percentage of micropores of 59.05%, has been produced from the ultra-pure lignite by microwave irradiation method with KOH and $ZnCl_2$ as activation agents, and presents a high specific capacitance of $170F \cdot g^{-1}$.

(2) When the active carbon is ultra-fine grinded to 2.1μm average size, the specific surface area will be improved to $1696m^2 \cdot g^{-1}$ with an increase of 10.4%, and the specific capacitance be improved to $184F \cdot g^{-1}$.

(3) The ultra-fine grinded and surface modification treated with SDBS active carbon has good wettability and presents a high specific capacitance of $189F \cdot g^{-1}$ and good cycle stability in KOH electrolytes.

(4) The synergistic effect of microwave irradiation, activation of KOH and $ZnCl_2$, ultra-fine grinding and surface modification have an obviously effect on preparing multiscale porous active carbon with appropriate pore-size distribution, developed micropore, sufficient mesopores and high micropore volume.

ACKNOWLEDGEMENTS

This work was partly supported by the Fundamental Research Funds for the Central Universities (2013XK07)

References

1. F. Béguin,E. Frąckowiak, *China Machine Press*, Beijing (2014).
2. X.X. Xiang, E.H. Liu, Z.Z. Huang, *J. Solid State Electrochem.*, 15 (2011) 2667.

3. Q. Fang, B.C. Yang, *Functional Materials*, 36(12) (2005) 1889.
4. A.B. Fuertes, *J. Mater. Chem*., 13 (2003) 3085.
5. D.W. Wang, F. Li and H.T. Fang, *J. Phys. Chem*. B, 110(17) (2006) 8570.
6. W. Lei, X. M. Zhao, P. He, H.T. Liu, *Chemical Bulletin*, 76(11) (2013) 981.
7. B.L. Xing, G.X. Huang, L.J. Chen, C.X. Zhang and L. Wang, *Journal of China Coal Society*, 38 (2013) 218.
8. Q. Xie, S.Q. Zhang, *Carbon Science and Technology*, 12(2) (2002) 24.
9. B.L. Xing, L.J. Chen, C.X. Zhang, *Journal of China Coal Society*, 36(7) (2011) 1200.
10. L. Han, K.X. Li, F. Gao, *Coal Conversion*, 31(3) (2008)71.
11. W.M. Chen, *Coal Science and Technology*, 2(6) (1994) 40.
12. H. Chen, Study on Electhode Materials of High Surface Area Activated Carbon with Different Pore Structures for Supercapacitor[D], Jilin: Northeast Normal University, 2011: 43.
13. B.L. Xing, L. Li, A.L. Ma, C.X. Zhang, L.J. Chen, *Materials review B: research papers*, 27(9) (2013)
14. F.K. Yuen, B.H. Hameed, *Adv. Colloid. Interf. Sci*., 149 (2009) 19.
15. J.T. Zhang, L.Y. Gong, K. Sun, J.C. Jiang, X.G. Zhang, *J. Solid State Electrochem*., 16 (2012) 2179.
16. X.F. Wang, D.Z. Wang, J. Liang, *Acta Phys.-Chim.Sin*., 18(8) (2002) 750.
17. J. Li, Y.Q. Lai, X.D. Jin, R.F. Peng, Y.X. Liu, *Chinese battery Industry*, 3(15) (2010) 131.
18. W. Xing, S.Z. Qiao, R.G. Ding, *Carbon*, 4(2) (2002) 216.
19. H. Yang, The Research on PreParation of Carbon Electrode Materials by Microwave Radiation for Supercapacitors[D], Changsha: Hunan University, 2007: 39.
20. W.F. Mu, Investigation of Surface Modification of Activated Carbon and Electrode Performance for Supercapacitor[D], Liaoning: Bohai University, 2012: 52.
21. J. F. Fauvarque and P. Simon, in Carbons for Electrochemical Energy Storage and Conversion Systems, F. Beguin and E. Frackowiak, Editor, CRC Press, Florida (2009) 29.
22. N.M. Thai, S.J. Kim, *J. Electrochem. Soc*., 162 (8) (2015) A1445
23. E. Frackowiak, F. Beguin, *Carbon*, 40 (2002) 1775
24. A. Balducci, R. Dugas, P.L. Tabema, *Power Sources*, 165(1) (2007) 922.
25. Z.G. Zhao, Application principle of adsorption, Chemical Industry Press, Beijing, 2005